Supplementary Table 1: Sequence parameters of the 3D high-resolution T_2^*-weighted gradient-echo sequence. Field of view and matrix size were adapted to the different tissue dimensions while maintaining the same spatial resolution.

Field of view	11 x 11 x 38 mm
Matrix size	157 x 157 x 190
Spatial resolution	0.07 x 0.07 x 0.200 mm
Repetition time	50 ms
Echo time	10 ms
Excitation pulse angle	12°
Number of averages	8
Scan time per acquisition	2 h 40 min

Supplementary Table 2: Contrast lesion-to-GM values with the corresponding myelin and inflammatory score for individual lesions. The type of lesions as well their volume (obtained by MRI) are also reported.

Animal	Lesion number	Type of lesions	Volume (mm^3)	Contrast (lesion-to-GM)	Myelin density score	Inflammatory cells score
M#1	1	focal	3.76	0.94	1	2
M#2	2	focal	0.34	0.92	1	1
M#3	3	focal	0.08	0.97	1	2
M#3	4	focal	0.03	0.94	1	2
M#3	5	focal	0.42	1.07	2	2
M#3	6	focal	1.38	1.02	2	2
M#3	7	focal	0.08	0.98	2	2
M#4	8	focal	0.03	0.96	2	1
M#4	9	focal	0.07	0.98	2	1
M#4	10	subpial	-	1.04	2	2
M#4	11	subpial	-	0.99	2	2

Supplementary Table 3: Results of the linear mixed-effect model M_2 showing the mean slope coefficient, standard error, and p-values by tissue type (***: $p \leq 0.001$)

Myelin model (M_2)	LFB	
MRI_{raw}	Slope (SE)	p-value
GM	56.3 (10.1)	2.2e-08***
Lesions	58.1 (8.2)	1.1e-12***
NAWM	17.3 (9.7)	0.07

Supplementary Figure 1

Preparation of spinal cord tissue for MRI. (A) The upper (left) and lower (right) spine are collected at necropsy, before cord extraction. (B) Four spinal cord pieces were obtained after extraction performed by a laminectomy (from the upper cervical on the left to the lower lumbo-sacral on the right). Note: the thoracic nerve roots (red arrow) were most easily preserved. (C) A 3D-printed model of the spinal cord holder was designed (Netfabb Professional 5.0 software, Autodesk Inc., San Rafael, CA, USA) with four slots to insert and align all portions of the cord. (D) Final spinal cord postmortem MRI setup, showing the spinal cord tissues restrained with cotton thread within the 3D-printed holder, which was subsequently inserted into a 15 ml tube. The holder was inserted into a 15 ml plastic tube and immersed in a proton-free, susceptibility-matched fluid (Fomblin, Solvay S.A, Brussels, Belgium). The same SC holder was used for all marmosets.

Supplementary Figure 2

Regions of interest drawn manually to compute the extent of subpial white matter lesions as a percentage of the total white matter. Light blue line: entire cross-section of the spinal cord; green line: edge of the NAWM; red line: GM.

Supplementary Figure 3

Example of regions of interests (black lines) manually drawn on the LFB-PAS (A) and propagated to the co-registered MRI (B) and LFB-deconvoluted gray level (C). ROIs were placed through the entire cord cross section to include NAWM, GM, and lesions.

Supplementary Figure 4

Areas of hemosiderin deposition within lesions of EAE animal M#2. The areas of hypointense signal on the MRI section match perfectly with the positive signal detected on Turnbull staining, which detects iron (red arrows). Note that these hemosiderin deposits may extend beyond areas of abnormal myelin, as shown on the Luxol fast blue-cresyl violet (LFB-CV) stain.

Supplementary Figure 5

The predicted MRI values from the mixed effects model M_2 versus the observed MRI values, as well as the corresponding regression line (blue). The coefficient of determination, R^2, is reported within the graphic. The black line corresponds to a perfect model fit with a $R^2 = 1$.

Supplementary Figure 6

T_2^*-weighted images from two different MRI sessions performed on the same spinal cord. (A) Before extraction of the cord from the spine. (B) After extraction. Red arrows point to areas of signal loss at the edges of the non-extracted spinal cord, some of which obscure subpial and focal lesions. This comparison shows why it is difficult to detect subpial pathology in the spinal cord on *in vivo* MRI.

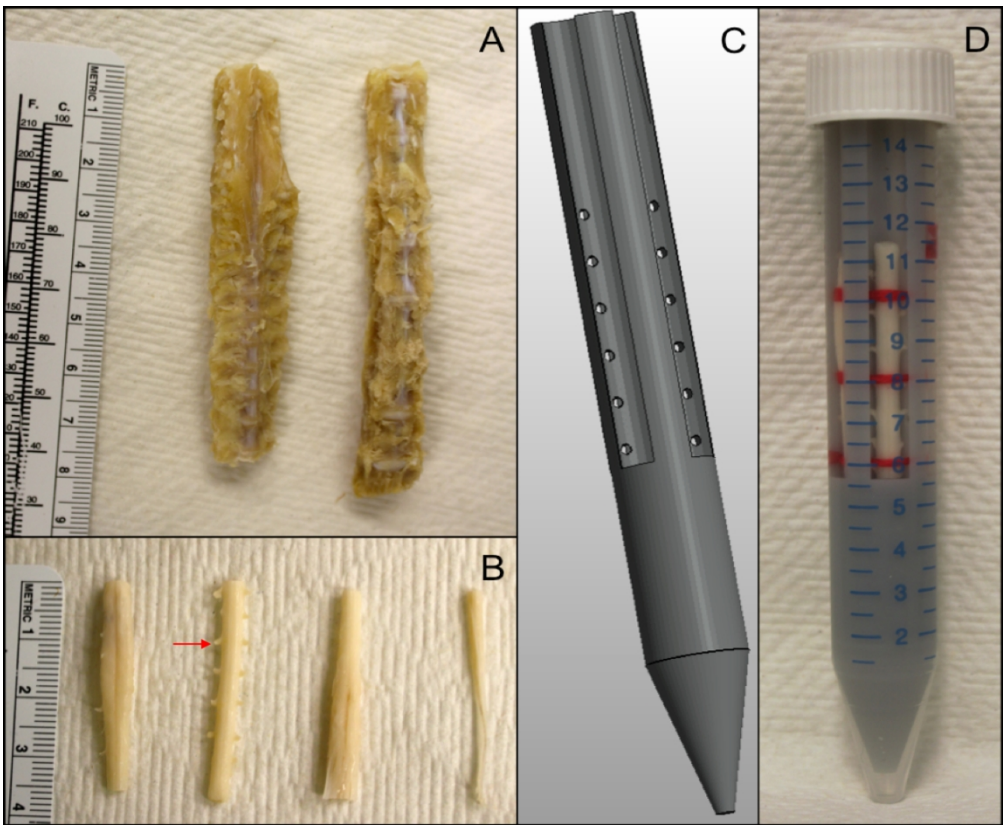

213x174mm (150 x 150 DPI)

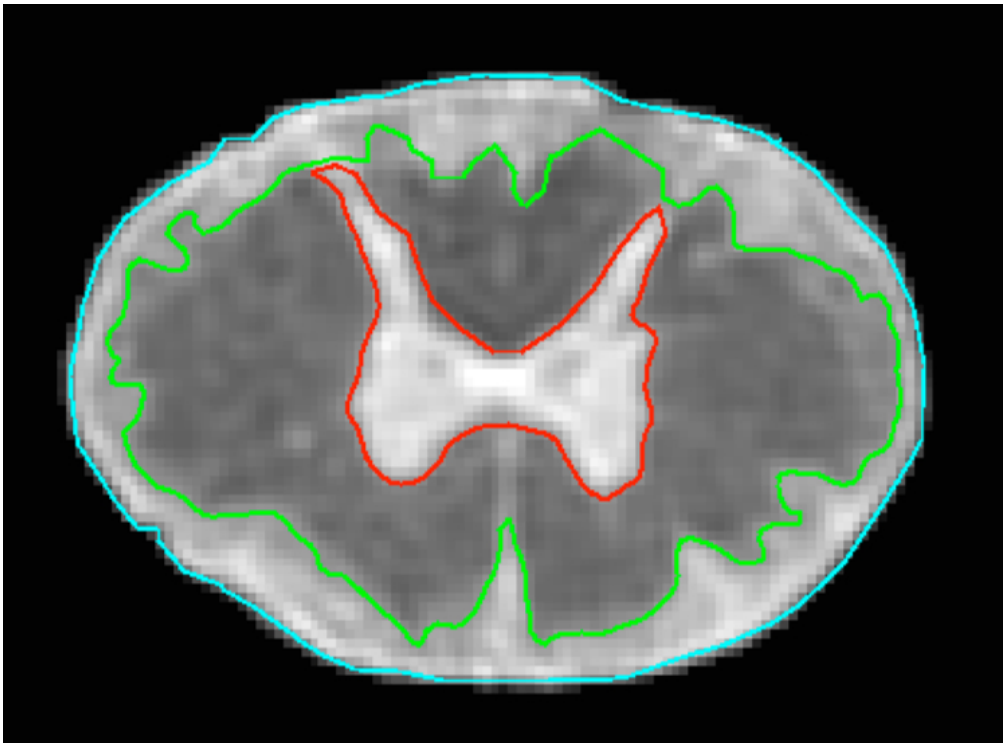

126x93mm (150 x 150 DPI)

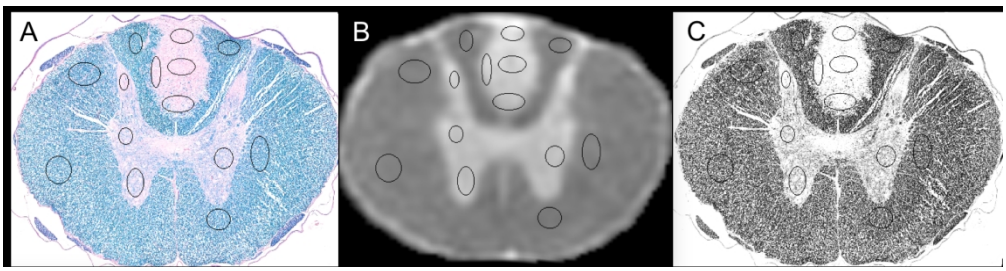

313x81mm (150 x 150 DPI)

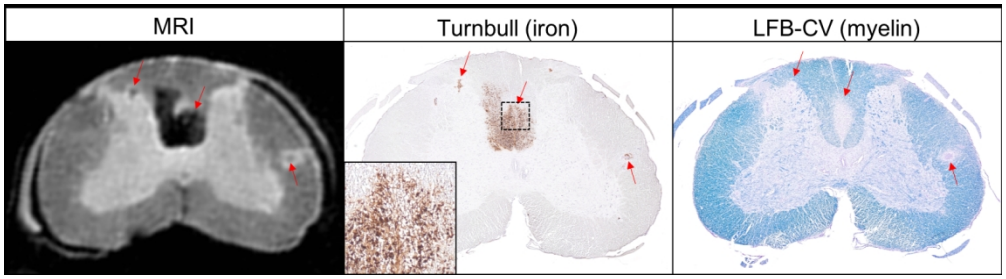
MRI
Turnbull (iron)
LFB-CV (myelin)

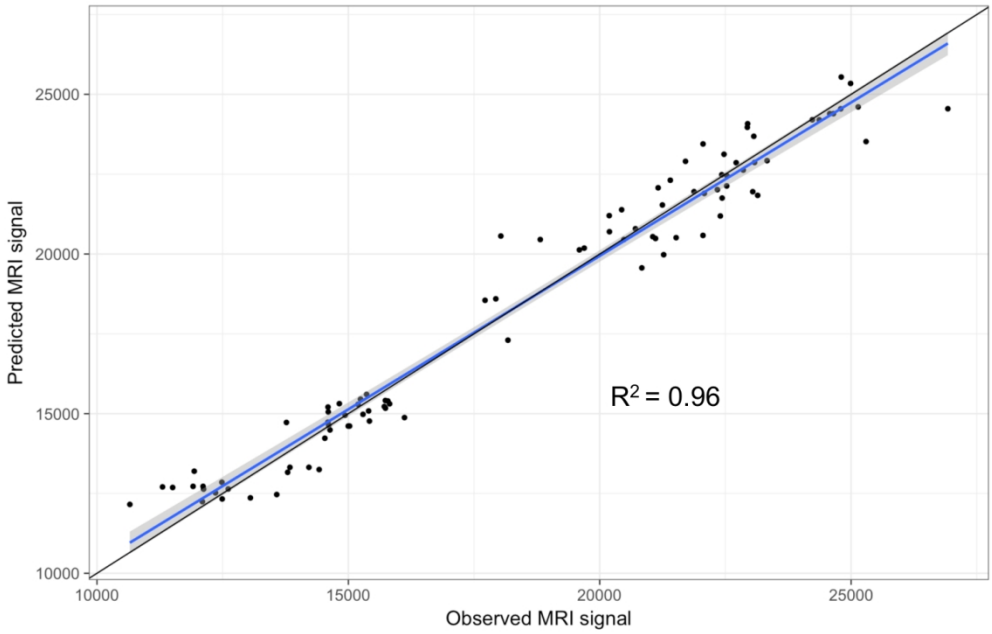

261x167mm (150 x 150 DPI)

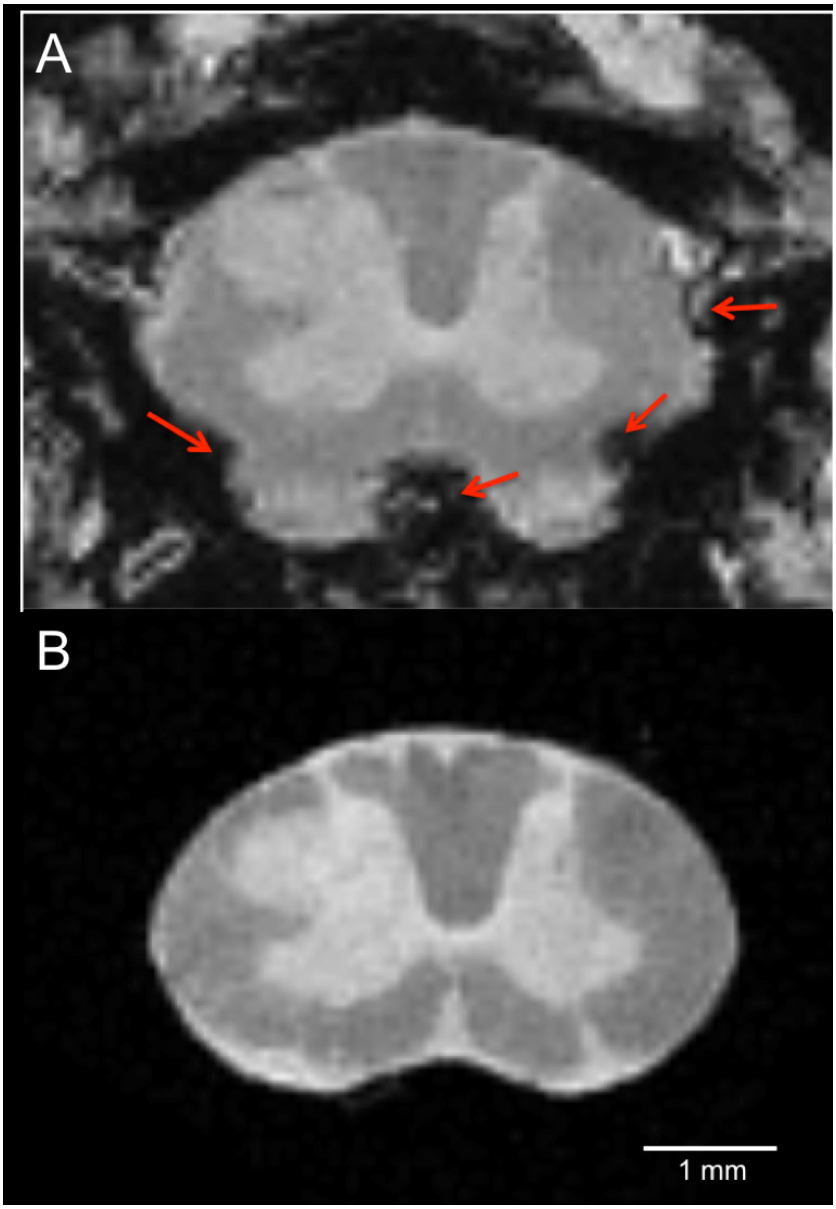

129x186mm (150 x 150 DPI)

Supplementary material: methods for histopathology

Luxol fast blue staining: sections were routinely deparaffinized and rehydrated, then incubated at 56˚C in LFB solution overnight. After washing excess stain with alcohol and distilled water, sections were differentiated in a 0.05% lithium carbonate solution followed by 70% ethyl alcohol. Sections were counterstained with periodic acid shift (PAS) solution.

Iba-1 immunohistochemistry: sections were routinely deparaffinized and rehydrated. Antigen retrieval was performed using steamer for 20 minutes in 0.01 M citrate buffer (pH 6). After washing with Tris-buffered saline, endogenous peroxidase activity was blocked with hydrogen peroxide (H_2O_2) for 10 min. Prior to primary antibody staining, nonspecific antibody binding was blocked by incubating with skim milk. Sections were incubated with a rabbit polyclonal Iba-1 (1:400; WAKO Pure Chemicals Ind., Osaka, Japan) for one hour at room temperature. After washing three times with Tris-buffered-tween 20, horseradish peroxidase (HRP)-conjugated secondary antibodies (Power vision, Leica, Wetzlar, Germany) were applied for 30 min at room temperature. The final reaction was performed by immersing the sections in a solution of 3,3'-Diaminobenzidine (DAB) (Abcam, Cambridge, UK). The sections were then counterstained with Mayer hematoxylin.

Turnbull's blue staining: sections were routinely deparaffinized and rehydrated, then immersed for 90 minutes in an aqueous 2% ammonium sulfide solution (Sigma Aldrich) for detection of total non-heme iron and washed with PBS. Sections were incubated within a solution of 10% potassium ferricyanide + 0.5% HCl during 15 minutes at 37˚ Celsius. After washing five times with distilled water, the sections were immersed in 0.3% hydrogen peroxide with methanol for 60 more minutes. Tissues were then washed with PBS and iron staining was amplified by DAB (Abcam, Cambridge, UK) until the adequate reaction was visualized and stopped by immersing within distilled water. Sections were counterstained with Mayer hematoxylin.